

# Visual cortex neurons in monkey and cat: Effect of contrast on the spatial and temporal phase transfer functions

DUANE G. ALBRECHT

Department of Psychology, University of Texas, Austin

(RECEIVED December 20, 1994; ACCEPTED May 8, 1995)

## Abstract

The responses of simple cells (recorded from within the striate visual cortex) were measured as a function of the contrast and the frequency of sine-wave grating patterns in order to explore the effect of contrast on the spatial and temporal phase transfer functions and on the spatiotemporal receptive field. In general, as the contrast increased, the phase of the response advanced by approximately 45 ms (approximately one-quarter of a cycle for frequencies near 5 Hz), although the exact value varied from cell to cell. The dynamics of this phase-advance were similar to the dynamics of the amplitude: the amplitude and the phase increased in an accelerating fashion at lower contrasts and then saturated at higher contrasts. Further, the gain for both the amplitude and the phase appeared to be governed by the magnitude of the contrast rather than the magnitude of the response. For the spatial phase transfer function, variations in contrast had little or no systematic effect; all of the phase responses clustered around a single straight line, with a common slope and intercept. This implies that the phase-advance was not due to a change in the spatial properties of the neuron; it also implies that the phase-advance was not systematically related to the magnitude of the response amplitude. On the other hand, for the temporal phase transfer function, the phase responses fell on five straight lines, related to the five steps in contrast. As the contrast increased, the phase responses advanced such that both the slope and the intercept were affected. This implies that the phase-advance was a result of contrast-induced changes in both the response latency and the shape/symmetry of the temporal receptive field.

**Keywords:** Visual cortex, Receptive field, Phase transfer function, Contrast, Spatial frequency, Temporal frequency

## Introduction

Over the past several decades (following the experiments of Hubel & Wiesel, 1962, 1968), the responses of neurons in the visual cortex of monkeys and cats have been measured as a function of the spatial frequency and the temporal frequency of drifting sine-wave grating patterns. These measurements result in a spatiotemporal transfer function, which is composed of an amplitude transfer function and a phase transfer function. A complete transfer function provides a systematic method for quantitatively characterizing some of the basic receptive-field properties of visual cortex neurons. Further, comparisons of the measured responses to those expected from a linear system are generally informative. (Progress within this general framework has been reviewed: e.g. Robson, 1975, 1983; Shapley & Lennie, 1985; De Valois & De Valois, 1988; Palmer et al., 1991; Skottun et al., 1991; DeAngelis et al., 1993; Jagadeesh et al., 1993; McLean & Palmer, 1994.)

In certain respects, the *phase transfer function* for simple cells is similar to the phase transfer function of a comparable bandpass linear filter. For such a filter, the phase of the response to drifting sine-wave gratings is determined by four different spatiotemporal properties of the filter: the spatial position, the spatial shape/symmetry, the temporal latency, and the temporal shape/symmetry (Hamilton, 1987; Hamilton et al., 1989). These four components add in a simple fashion such that the spatiotemporal phase transfer function can be described using a pair of linear equations, with the four parameters determined by the four spatiotemporal properties of the filter. Hamilton et al. (1989) have shown that these linear equations provide a good description of the measured phase transfer function of visual cortex simple cells (recorded from both cat and monkey) and that the four parameters provide a quantitative metric for describing the spatial and temporal properties of the receptive field. (For related work on the phase transfer function in the retina, lateral geniculate nucleus, and the visual cortex, see Shapley & Victor, 1978, 1979, 1981; Lee et al., 1981*a,b*; Enroth-Cugell et al., 1983; Dawis et al., 1984; Hamilton, 1987; Reid et al., 1992.)

Reprint requests to: Duane G. Albrecht, Department of Psychology, University of Texas, Austin, TX 78712, USA.

In other respects, the phase transfer function for simple cells is different from the phase transfer function of a linear filter. In a linear filter, the phase of the response is not affected by contrast. For simple cells, the phase of the response advances as the contrast is increased (Albrecht, 1978; Dean & Tolhurst, 1986; Carandini & Heeger, 1994), similar to neurons in the retina (Shapley & Victor, 1978, 1979, 1981) and the lateral geniculate nucleus (Sclar, 1987).

The first aim of the research reported here was to provide a more thorough understanding of the contrast-induced phase-advance, and if possible, to characterize the contrast-phase relationship with a quantitative mathematical formulation. Previous work has shown that the Naka-Rushton relationship provides a good description of the response amplitude as a function of contrast (Albrecht & Hamilton, 1982; Albrecht & Geisler, 1991; Sclar et al., 1990; Geisler & Albrecht, 1992, 1995; DeAngelis et al., 1993). The results of the present analysis show that the same relationship provides a good description of the response phase as a function of contrast. Thus, the descriptive parameters of this equation were utilized to compare the dynamics of the amplitude with the dynamics of the phase, and to summarize the sample of cells as a whole.

The second aim of this study was to explore the effect of contrast on the spatiotemporal receptive-field properties. To this end, the spatiotemporal phase transfer function was measured at multiple contrasts. As noted above, when measured at a fixed contrast, the phase transfer function is adequately described by linear equations with four parameters, and each parameter is individually influenced by a specific receptive-field property. For the spatial phase transfer function, the slope is determined by the spatial position of the receptive field and the intercept is determined by the spatial shape/symmetry of the receptive field. (Related work on these properties of the receptive fields can be found in Pollen & Ronner, 1981; Field & Tolhurst, 1986; Hawken & Parker, 1987; Jones & Palmer, 1987; Ferster, 1988.) For the temporal phase transfer function, the slope is determined by the temporal latency and the intercept is determined by the temporal shape/symmetry of the receptive field. (Related work on these properties of the receptive fields can be found in Lee et al., 1981*a,b*; Lennie, 1981; Reid et al., 1992; DeAngelis et al., 1993.) Therefore, by measuring the slopes and the intercepts of the spatial and temporal phase transfer functions at multiple contrasts, it should be possible to determine what aspect of the space-time receptive-field changes as a function of contrast. The results of the analysis imply that variations in contrast produce a change in both the latency and the shape/symmetry of the temporal receptive field.

The third aim of this study was to evaluate the effects of contrast on the phase transfer function, within the context of other known properties of the contrast response function of visual cortex neurons. Previous work has shown that as contrast increases, the response amplitude for most cortical cells increases over some range of contrasts and then remains static, at a maximum saturated value; further, the point of saturation in the contrast response function is not determined by the overall magnitude of the response, but rather by the overall magnitude of the contrast (Albrecht & Hamilton, 1982; Sclar & Freeman, 1982; Li & Creutzfeldt, 1984; Skottun et al., 1987; Albrecht & Geisler, 1991, 1994; Bonds 1991, 1993; Geisler & Albrecht, 1992, 1995; Heeger, 1992*a*; Carandini & Heeger, 1994; see Appendix). In the present analysis, the phase transfer function was measured at multiple contrasts to determine whether the phase-

advance was a consequence of the magnitude of the contrast, the magnitude of the response, or both. The results of the analysis imply that the phase-advance was primarily determined by the overall level of the contrast and not the overall level of the response.

## Methods

Procedures for the electrophysiological recording, the display of stimuli, and the measurement of neural responses using linear systems analysis have been described (Albrecht & Hamilton, 1982; Albrecht et al., 1984; Hamilton et al., 1989; Albrecht & Geisler, 1991; Geisler et al., 1991). The stimuli were drifting spatiotemporal sine-wave grating patterns presented on a Conrac studio monitor. The mean luminance was held constant at 27.4 cd/m<sup>2</sup>. Contrast (Michelson contrast) was defined as  $100 \cdot (L_{\max} - L_{\min}) / (L_{\max} + L_{\min})$ . Both hardware and software methods were utilized to compensate for display nonlinearities.

The contrast, spatial frequency, temporal frequency, and direction of stimulus motion were varied in a systematic fashion, such that each of the different stimulus conditions were randomly interleaved. One presentation at a fixed spatiotemporal contrast consisted of a block of 10 or 12 contiguous temporal cycles. Each block was separated by a period of time equal to the block length; during these separations, the contrast was zero. Thus, for example, for the responses shown in Fig. 1, 12 contiguous temporal cycles were presented at one contrast, followed by zero contrast, followed by a randomly selected second contrast, followed by zero contrast, etc. Similarly, for the responses shown in Fig. 10, a given spatiotemporal frequency was drifted in one direction, followed by zero contrast, followed by a second randomly selected spatiotemporal frequency, direction, etc. A minimum of four blocks were obtained for each stimulus condition, which resulted in 40 or 48 repeated temporal cycles. Action potentials were collected in 0.1-ms time bins and the resulting spike trains were then Fourier analyzed. Once a single neuron had been isolated and classified as a simple cell, its optimal orientation was determined and held constant throughout the experiment.

### Analysis of the contrast response functions

The responses as a function of contrast,  $R(C)$ , were fitted to the Naka-Rushton equation using least-squares criteria:

$$R(C) = R_{\max} C^n / (C^n + C_{50}^n) \quad (1)$$

The amplitude and the phase of the first harmonic component were fitted separately. When  $R(C)$  refers to the amplitude of the response as a function of contrast,  $R_{\max}$  is the maximum saturated response,  $C_{50}$  is the contrast that evoked 50% of  $R_{\max}$ , and  $n$  is the power function exponent.\* When  $R(C)$

\*In comparison to neurons in the retina and LGN, neurons in the visual cortex have a rather low spontaneous discharge. The spontaneous discharge for most simple cells is generally much less than one action potential per second. Further, this spontaneous discharge is generally not rhythmically periodic at the fundamental frequency of the stimulus. Thus, there is generally little or no spontaneous activity at the amplitude of the first harmonic of the stimulus. However, whenever there was spontaneous activity at the first harmonic, it was subtracted from the responses prior to fitting eqn. (1).

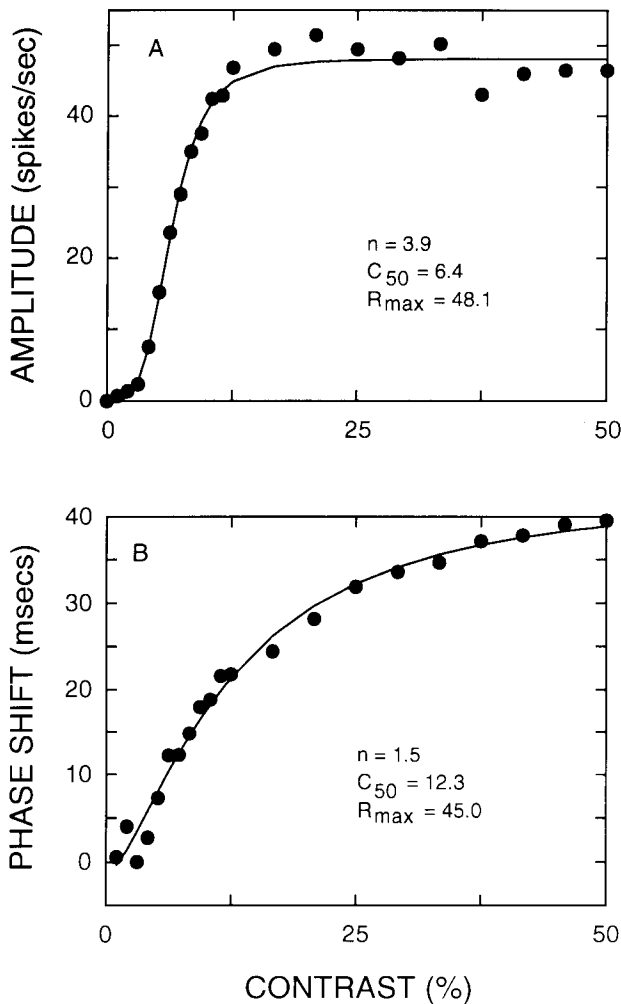


**Fig. 1.** Contrast response function for a representative neuron, recorded from within the visual cortex of a cat. The stimulus was a drifting sine-wave grating pattern (at the optimal spatial and temporal frequency, 0.44 cycle/deg, 6.25 cycle/s), presented at various contrasts. In (A), the amplitude of the response of the first harmonic component is plotted as a function of contrast. The smooth curve through the measured responses is the best fit of the Naka-Rushton relationship [see eqn. (1)]; the optimized values of the three parameters are listed. As the contrast increased, the response increased and then saturated. In (B), the phase of the response is plotted as a function of contrast. The phase responses are expressed as a shift in time (milliseconds), relative to the lowest value. The smooth curve through the measured responses is the best fit of the Naka-Rushton relationship [see eqn. (1)]; optimized values of the three parameters are listed. As the contrast increased, the phase of the response advanced (or shifted) in time. So, for example, the response of the cell to a 30% contrast occurred approximately 30 ms sooner than the response of the cell to a 3% contrast. The phase and the amplitude of the contrast response function were similar (the phase and the amplitude were dynamic at lower contrasts and static at higher contrasts), although not identical.

refers to the phase of the response as a function of contrast,  $R_{max}$  is the maximum saturated phase,  $C_{50}$  is the contrast that evoked 50% of  $R_{max}$ , and  $n$  is the power function exponent.

For the results presented in Part I of this study, the spatial frequency and the temporal frequency were held constant at, or near, the optimal values for each cell and the phase as a function of contrast data (e.g. Figs. 1–9) were normalized across cells

by expressing the phase responses as a shift in time (in ms) relative to the lowest value. Alternatively, the shift can be expressed as a fraction of the period of the stimulating temporal frequency (in degrees, or in  $\pi$  radians); the normative statistics were summarized in this fashion at the end of Part I and in the discussion section.† For the sample of cells as a whole, the stimulating temporal frequency ranged from 1–10 Hz. For nearly 75% of the cells, the stimulating temporal frequency fell within a range of 4.0–8.0 Hz. The average stimulating temporal frequency was 5.5 Hz, for both cat and monkey.

*Analysis of the phase transfer function*

*The four-parameter linear model*

Consider measuring the response of a linear filter, with band-pass spatiotemporal characteristics similar to a simple cell (e.g. a linear quadrature spatiotemporal filter, Watson & Ahumada, 1983, 1985; Adelson & Bergen, 1985), as a function of time.‡ The measured phase response,  $P$ , at a particular spatial frequency,  $\mu$ , and temporal frequency,  $\omega$ , can be described by the following equation (Hamilton, 1987; Hamilton et al., 1989):

$$P(\mu, \omega) = \text{sgn}(\mu)\theta_s - \mu p + \text{sgn}(\omega)\theta_t - \omega l \quad (2)$$

Eqn. (2) generates a pair of straight lines. One line describes the spatial phase transfer function, with slope  $p$  and intercept  $\theta_s$ ; the other line describes the temporal phase transfer function, with slope  $l$  and intercept  $\theta_t$ . The phase symmetries about the spatiotemporal origin are introduced by the  $\text{sgn}$  function, which is +1 for positive frequencies and -1 for negative frequencies.

These four parameters correspond to four separate properties of the spatiotemporal filter.

1. The *spatial position* of the filter introduces a fixed spatial displacement and thus a phase shift which increases with spatial frequency; the spatial position of the filter is given by the slope of the spatial phase transfer function ( $p/360$  deg).
2. The *spatial phase* of the filter (the spatial shape/symmetry) introduces a fixed phase shift independent of frequency; the spatial phase of the filter is given by the intercept of the spatial phase transfer function ( $\theta_s$ ).

†Consider the potential effect of the stimulating temporal frequency on these conventions within the framework of the four-parameter model of the phase transfer function. When the phase-advances are expressed as a fixed delay in time then any changes in the latency (as a function of contrast) should have a constant effect, independent of stimulating temporal frequency, while any changes in the shape/symmetry (as a function of contrast) should have a larger effect as the temporal frequency decreases. Conversely, when the phase-advances are expressed as a fixed fraction of the period of the stimulating temporal frequency (in degrees, or  $\pi$  radians) then any changes in the latency (as a function of contrast) should have a larger effect as the stimulating temporal frequency increases, while any changes in the shape/symmetry (as a function of contrast) should have a constant effect, independent of frequency.

‡It is easy to show that the phase transfer function of a bandpass linear filter similar to a simple cell can be adequately described by eqn. (2). For example, eqn. (2) would describe the phase transfer function of a bandpass Gabor-like filter (i.e. the product of a cosine and a Gaussian). However, it is important to note that the phase transfer function of a linear filter at very low frequencies may not be adequately described by eqn. (2) (see Hamilton et al., 1989, p. 1299).

3. The *temporal latency* of the filter introduces a fixed delay in time, and thus a phase shift which increases with temporal frequency; the temporal latency of the filter is given by the slope of the temporal phase transfer function ( $l/360$  deg).
4. The *temporal phase* of the filter (the temporal shape/symmetry) introduces a fixed phase shift independent of frequency; the temporal phase of the filter is given by the intercept of the temporal phase transfer function ( $\theta_t$ ).

#### The phase symmetries

Gratings drifting in the preferred direction of motion were treated as positive spatiotemporal frequencies: positive spatial frequencies and positive temporal frequencies,  $P(\mu, \omega)$ . Gratings drifting in the nonpreferred direction were treated as negative spatiotemporal frequencies: negative spatial frequencies and positive temporal frequencies,  $P(-\mu, \omega)$ . Following from this convention, the temporal components combine in an even-symmetric fashion about the origin (i.e. they add for motion in either direction) and the spatial components combine in an odd-symmetric fashion about the origin (i.e. they add for motion in one direction and subtract for motion in the other direction).

Thus, the spatial phase transfer function is the difference of the responses in each direction divided by 2, and the temporal phase transfer function is the sum of the responses in each direction, divided by 2. Specifically, when the phase responses to gratings drifting in the nonpreferred direction are subtracted from the phase responses to gratings drifting in the preferred direction, the temporal components cancel, leaving only the spatial components. Dividing by 2 results in  $P_g(\mu)$ , the spatial phase transfer function:

$$P_g(\mu) = [P(\mu, \omega) - P(-\mu, \omega)]/2 \quad (3)$$

When eqn. (2) holds, this simplifies to

$$P_g(\mu) = \theta_s - \mu p \quad (4)$$

Similarly, when the phase responses to gratings drifting in the nonpreferred direction are summed with the phase responses to gratings drifting in the preferred direction, the spatial components cancel leaving only the temporal components. Dividing by 2 results in  $P_h(\omega)$ , the temporal phase transfer function:

$$P_h(\omega) = [P(\mu, \omega) + P(-\mu, \omega)]/2 \quad (5)$$

When eqn. (2) holds, this simplifies to

$$P_h(\omega) = \theta_l - \omega l \quad (6)$$

## Results

### Part I: A description of the contrast-induced phase advance

The first goal of this study was to provide a general qualitative and quantitative description of how the temporal phase of the response to sine-wave gratings varies as a function of contrast. To that end, the responses of 136 neurons identified as simple cells were measured as a function of contrast (116 neurons were recorded from within cat striate cortex, and 20 neurons were recorded from within macaque striate cortex).

The responses of a representative cell are shown in Fig. 1. The upper graph (Fig. 1A) shows the amplitude of the response; the smooth curve through the data points is the best fit of the Naka-Rushton function [a saturating power function, given in eqn. (1)]. The behavior of this cell is typical of this sample and is consistent with what has been reported (e.g. Albrecht & Hamilton, 1982; Sclar et al., 1990; DeAngelis et al., 1993). Specifically, as the contrast increased, the amplitude of the response increased at an accelerating rate with a power function exponent greater than 1 ( $n = 3.9$ ). Then, as the contrast was increased beyond the semi-saturation contrast ( $C_{50} = 6.4\%$  contrast), the growth in the amplitude diminished and the response approached the saturated maximum level ( $R_{\max} = 48.1$  spikes/s).

The lower graph (Fig. 1B) shows the phase-shift of the response as a function of luminance contrast; the vertical axis plots any relative phase-advance in milliseconds. The smooth curve through the data points is the best fit of the Naka-Rushton function, applied to the phase responses. As can be seen, there was a clear and consistent relationship between the contrast and the phase. Specifically, as the contrast increased, the phase-shift increased, with a power function exponent greater than 1 ( $n = 1.5$ ). Then, as the contrast was increased beyond the semi-saturation contrast ( $C_{50} = 12.3\%$  contrast), the growth in the phase diminished and the phase approached the saturated maximum level ( $R_{\max} = 45.0$  ms). In other words, as the contrast increased, the phase advanced and thus the response occurred sooner; the delay in time between the onset of the stimulus and the onset of the response decreased. For this cell, the response to a high contrast stimulus occurred approximately 45 ms sooner than the response to a low contrast stimulus.

It is worth comparing the dynamics of the amplitude with the dynamics of the phase. For the cell shown in Fig. 1, the dynamics of the amplitude and the phase were similar although not identical. Consider first the power function exponents: although the exponents were expansive for both the amplitude and the phase, the exponent for the amplitude function was larger. Consider next the semi-saturation contrasts: although the semi-saturation contrasts were both less than 15%, the semi-saturation contrast of the amplitude function was smaller.

Similar measurements of the amplitude and the phase of the response are shown in Fig. 2 for two cells recorded from the cat visual cortex and in Fig. 3 for two cells recorded from the monkey visual cortex. For each cell, the amplitude of the response is plotted above the phase of the response, and the smooth curves show the fits of eqn. (1), with the optimized parameters as listed. These four cells are representative of the sample and they illustrate the basic trends in the data. The amplitude and the phase for each cell were similar, although not identical. Specifically, both were generally expansive at lower contrasts and compressive at higher contrasts; the functions increased rapidly with expansive exponents and then saturated. However, the exact values of the optimized parameters for the amplitude and phase were not identical.

The responses of the neurons illustrated in Figs. 1-3 are representative of the sample: the phase of the response advanced as a function of contrast. There were only four exceptions to this rule. The phase responses for three neurons recorded in the cat and one neuron recorded in the monkey shifted in the opposite direction (i.e. contrast introduced a phase-lag); these four neurons have been excluded from subsequent analyses within this report.

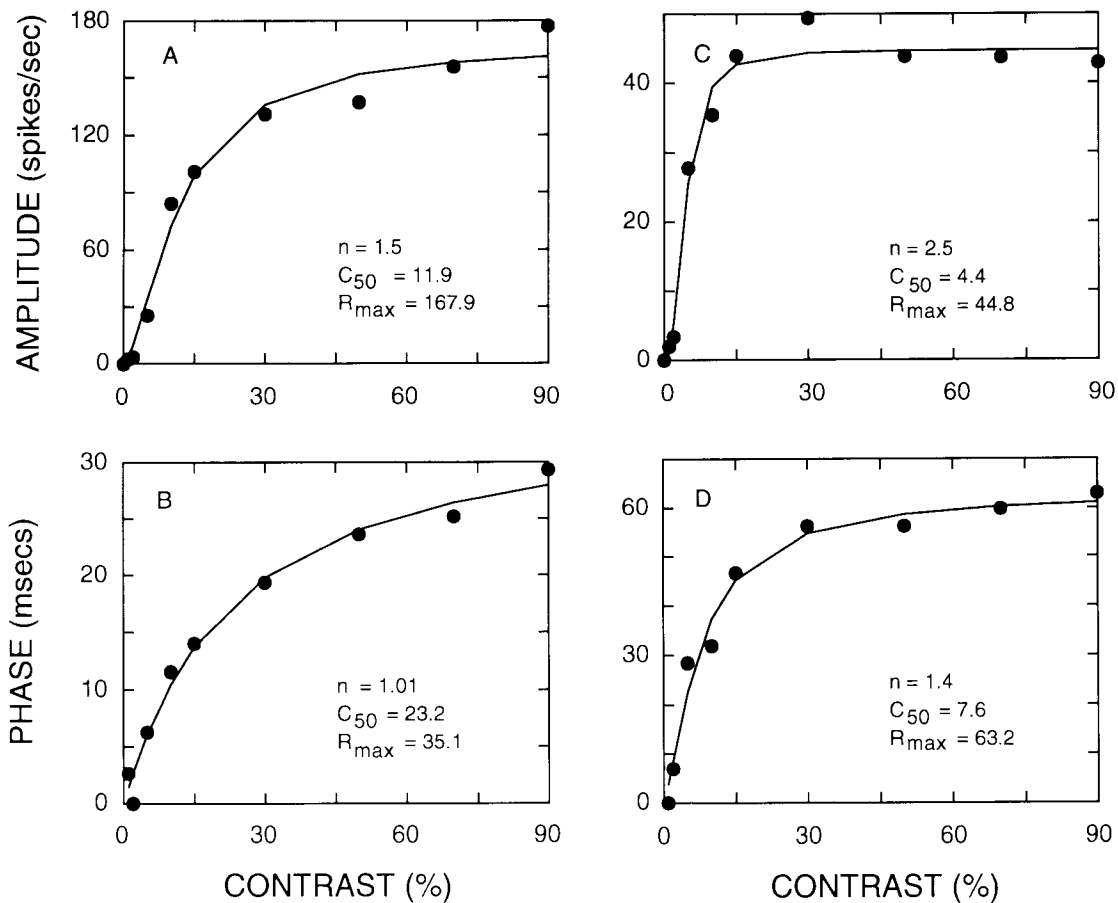


**Fig. 2.** Contrast response function for two representative neurons recorded within the cat visual cortex. The amplitude and phase of the response are plotted as a function of contrast, as described in the caption for Fig. 1. The stimulus was a drifting sine-wave grating pattern (0.44 cycle/deg, 10.0 cycle/s for A and B; 0.67 cycle/deg, 4.0 cycle/s for C and D), presented at various contrasts. The smooth curve is the best fit of eqn. (1), with the optimized parameters as indicated.

The parameters of the Naka-Rushton function provide a quantitative method for describing the entire sample of neurons. The distributions of the power function exponents for both cat and monkey are shown in Fig. 4; the exponents for the amplitude functions are shown above the phase functions. As can be seen, for this sample of neurons there was a wide range of possible exponents, from less than 1 to greater than 7, and the distributions were similar. Nevertheless, for the population of cat cells, the average value of the exponent for the phase function was slightly larger than the average value of the exponent for the amplitude function. For the population of monkey cells, the trend was in the same direction.

Scatter plots of the amplitude and phase exponents for each cell are shown in Fig. 5. The exponent for the amplitude function is plotted along the horizontal axis and the exponent for the phase function is plotted along the vertical axis. These scatter plots show that the expansive power function exponents were not correlated. This was true for both the cat cells and the monkey cells.

The distributions of the semi-saturation contrasts for the cat and monkey amplitude and phase functions are shown in Fig. 6. The distributions of amplitude vs. phase were quite similar within species. Scatter plots of the amplitude and phase semi-

saturation contrasts for each cell are shown in Fig. 7. There was a positive correlation of 0.51 for the cat cells and 0.81 for the monkey cells.

The  $R_{max}$  parameter provides an index of the overall magnitude of the phase-advance; the distributions for cat and monkey are shown in Fig. 8. These distributions show that for some cells the phase-advance was less than 10 ms, while for other cells the phase-advance was larger than 70 ms. The average value of the phase-advance was approximately 40 ms for the cat cells and 50 ms for the monkey cells.

One method for summarizing the general trends for the entire sample of cells is to simply average the amplitude and the phase of the contrast response functions, across all of the cells measured; the results of performing this operation are shown in Fig. 9. Each data point is the average response, and the smooth curves are the best fits of eqn. (1), with the parameters listed.

All of the measurements described above were performed at, or near, the optimal temporal frequency for each cell and the phase responses were normalized across cells by expressing the phase-advance as a shift in time (in milliseconds), relative to the lowest value. Alternatively, the phase-advance can be expressed as a fixed fraction of the period of the stimulating temporal frequency, in degrees or in  $\pi$  radians. Thus, for exam-

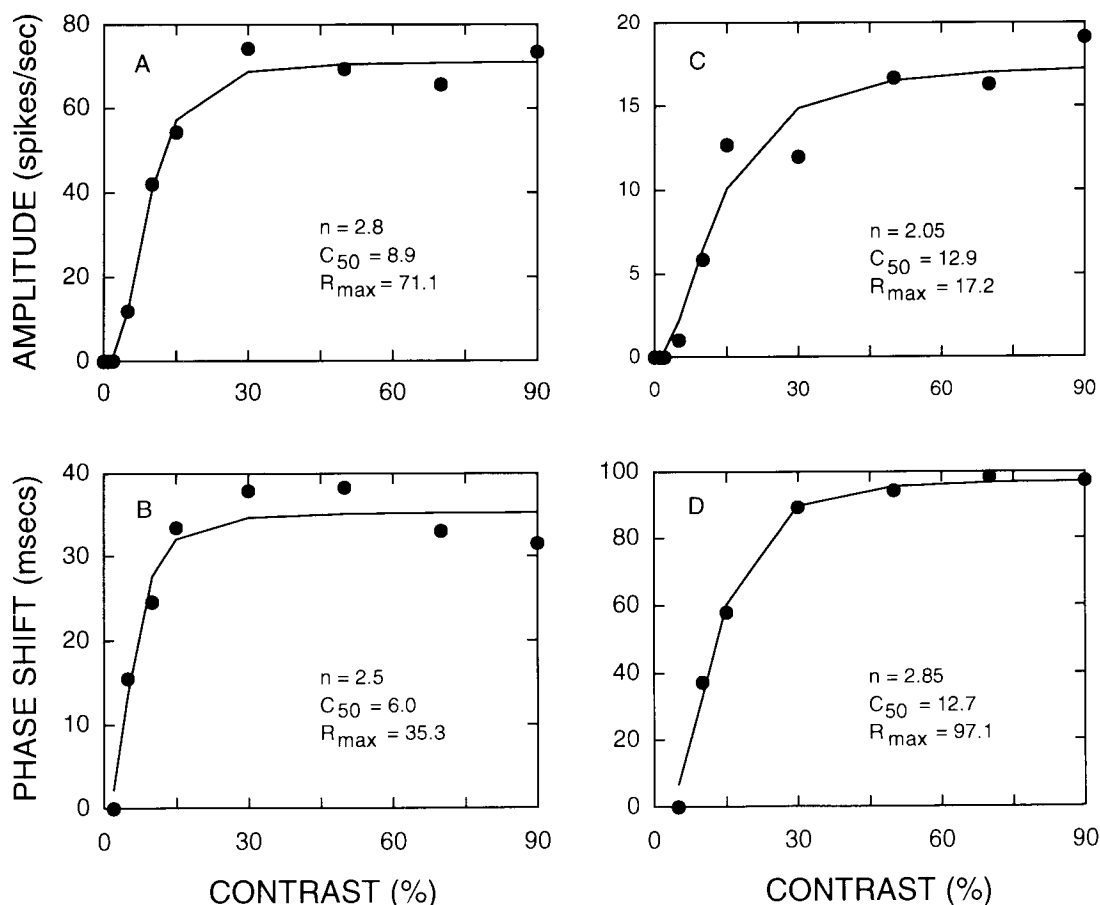


**Fig. 3.** Contrast response function for two representative neurons recorded within the monkey visual cortex. The amplitude and phase of the response are plotted as a function of contrast as described in the caption for Fig. 1. The stimulus was a drifting sine-wave grating pattern (1.33 cycle/deg, 5.0 cycle/s for A and B; 1.67 cycle/deg, 6.0 cycle/s for C and D), presented at various contrasts. The smooth curve is the best fit of eqn. (1), with the optimized parameters as indicated.

ple the phase-advance for the cell shown in Fig. 1, as indexed by the  $R_{\max}$  parameter, was  $0.56 \pi$  radians of the 6.25 cycles/s stimulating temporal frequency (i.e. approximately one-quarter of the period). For the sample of cells as a whole (averaging across both cat and monkey), the average phase-advance over a contrast range of 1–90% was  $0.42 \pi$  radians.

A scatter plot of the phase-advances along with the stimulating temporal frequencies ( $\pi$  radians along the vertical axis and cycles/s along the horizontal axis) shows that for this sample of cells there was a wide range of phase-advances at each of the different stimulating temporal frequencies. For example, there were phase-advances smaller than  $0.3 \pi$  radians and greater than  $0.7 \pi$  radians over a range which extended from 2–10 Hz. Nevertheless, there was a positive correlation of 0.24, with a slope of 0.034 and an intercept of 0.23. This interaction could potentially result from a number of different factors, including changes in both the latency and the shape/symmetry of the temporal receptive field (see footnote † on p. 1193).

#### *Part II: The effect of contrast on the phase transfer function*

The second goal of this study was to investigate the relationship between the phase-advance and the spatiotemporal prop-

erties of the receptive field. To that end, the spatiotemporal phase transfer function was measured at multiple contrasts.

Previous work has demonstrated that when the phase transfer function of simple cells is measured at a fixed contrast, it is similar to the phase transfer function of a comparable band-pass linear filter (Hamilton et al., 1989). Specifically, the spatiotemporal phase responses of simple cells are symmetric for gratings drifting in the preferred vs. nonpreferred direction of motion. Further, they can be described using a pair of straight lines with four parameters [see eqn. (2)]. The phase responses as a function of spatial frequency are odd-symmetric about the origin and thus can be described using a single slope parameter and a single intercept parameter. Similarly, the phase responses as a function of temporal frequency are even-symmetric about the origin and thus can be described with a single slope parameter and a single intercept parameter.

Fig. 10 shows the spatiotemporal transfer function for a representative neuron measured at a fixed contrast; the amplitude and the phase of the response are plotted as a function of the spatial frequency and the temporal frequency for gratings drifting in the preferred direction of motion and for gratings drifting in the nonpreferred direction of motion. The straight lines through the phase responses show the fit of the four-parameter linear phase relationship [given in eqn. (2)]; the responses across

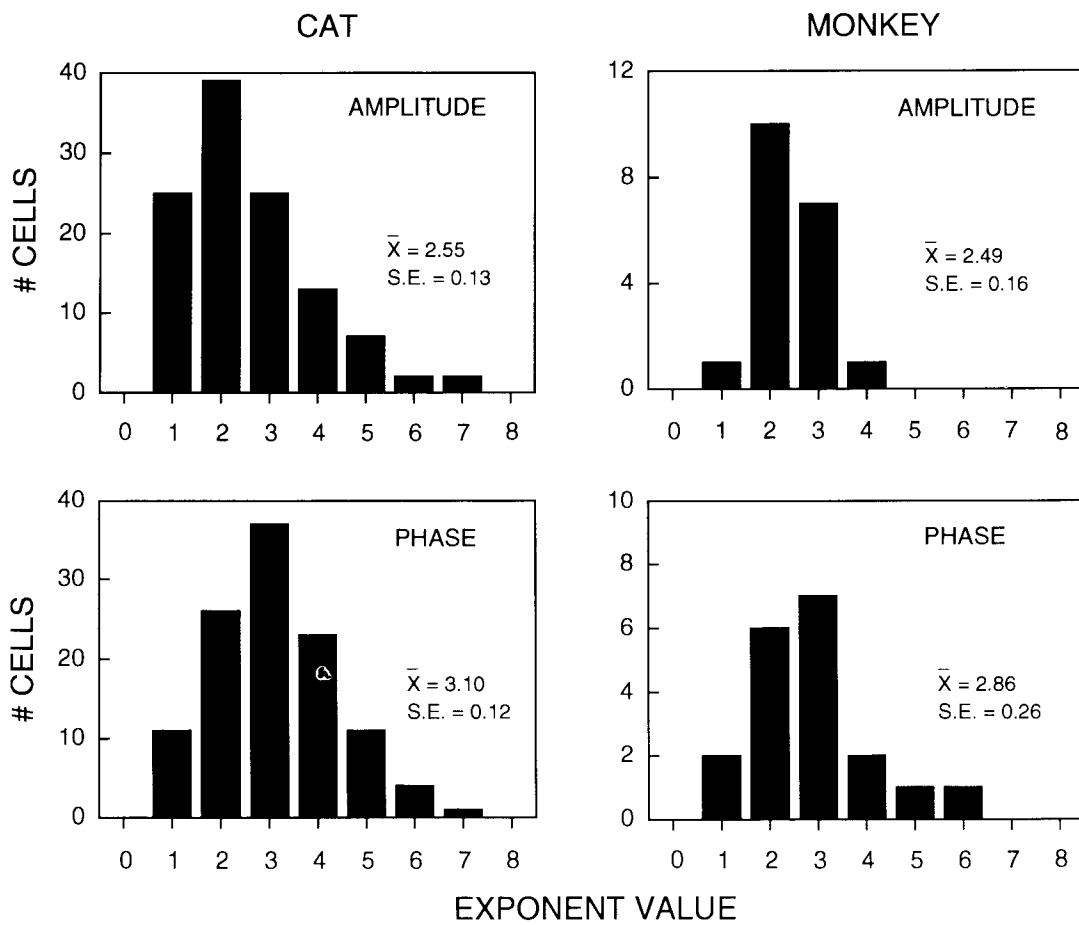


Fig. 4. Distributions of the exponent parameter,  $n$ , of the Naka-Rushton relationship [eqn. (1)], for the phase and the amplitude responses for the total sample of cells. The mean and the standard error are listed alongside each distribution. All four distributions were similar in terms of their means and in terms of the ranges of values covered.

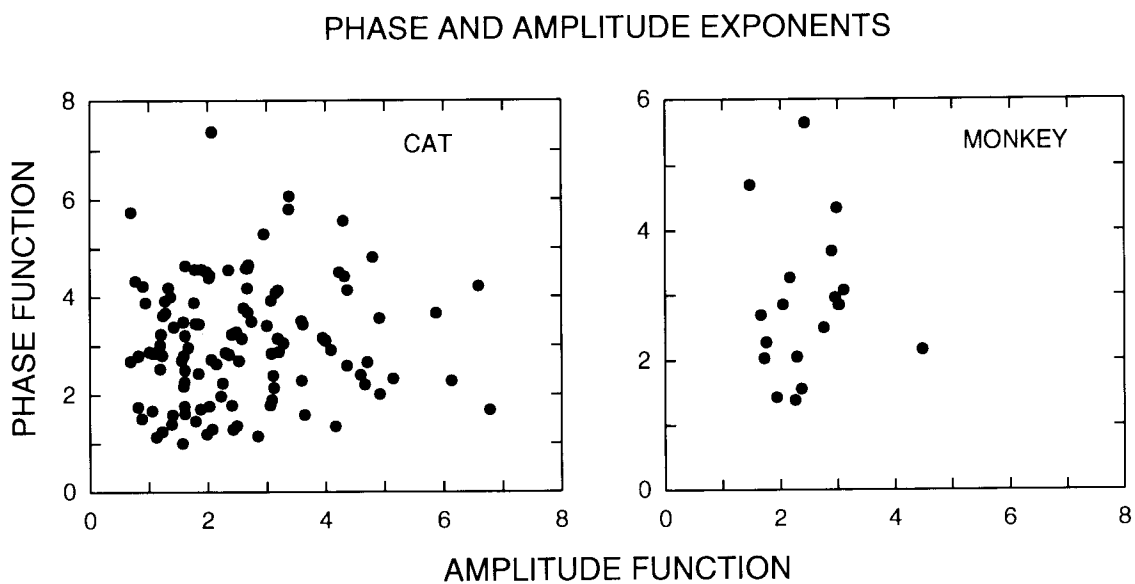


Fig. 5. Scatter plots for the phase and amplitude exponents for the entire sample of cells. Each point plots the phase and amplitude exponents for one cell. The amplitude exponents are plotted along the horizontal axis and the phase exponents are plotted along the vertical axis. There was little or no correlation.

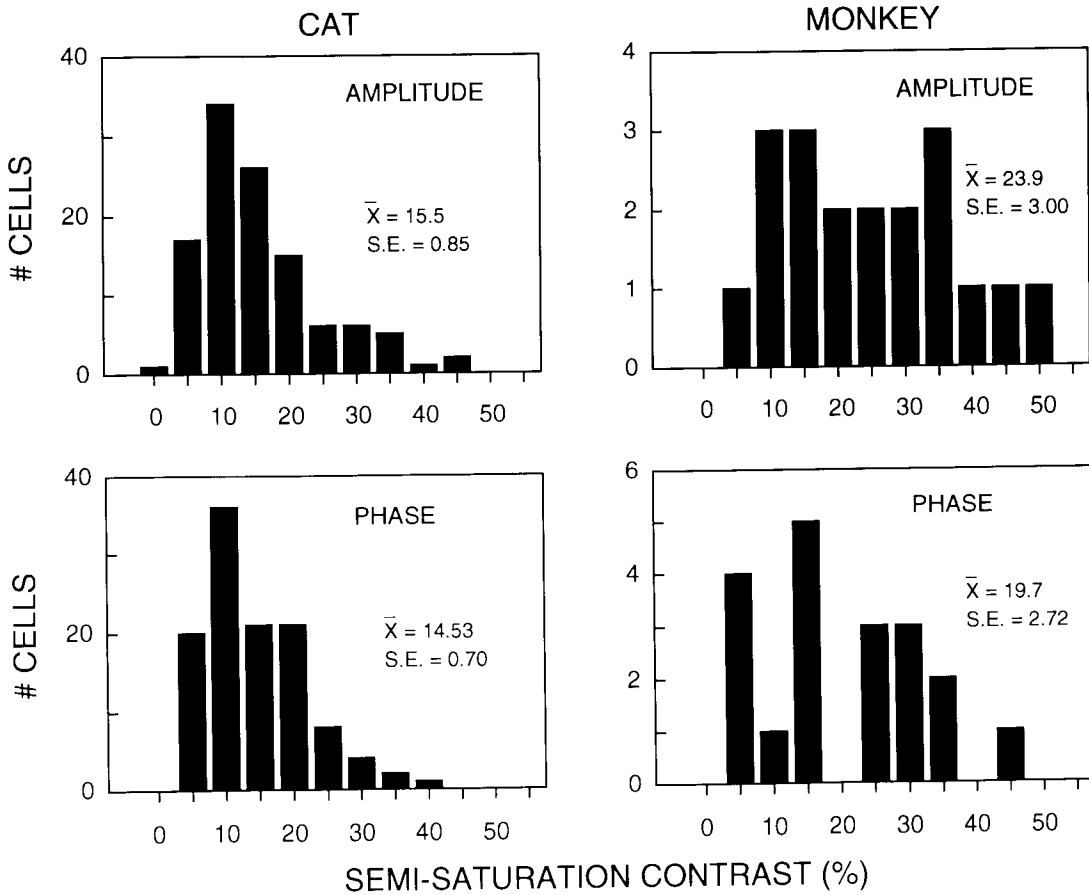


Fig. 6. Distributions of the semi-saturation parameter,  $C_{50}$ , of the Naka-Rushton relationship [eqn. (1)], for the phase and the amplitude responses for the entire sample of cells. The mean and the standard error are listed alongside each distribution. All four distributions were similar in terms of their means and in terms of the ranges of values covered; however, the cells recorded from monkey were shifted to larger values.

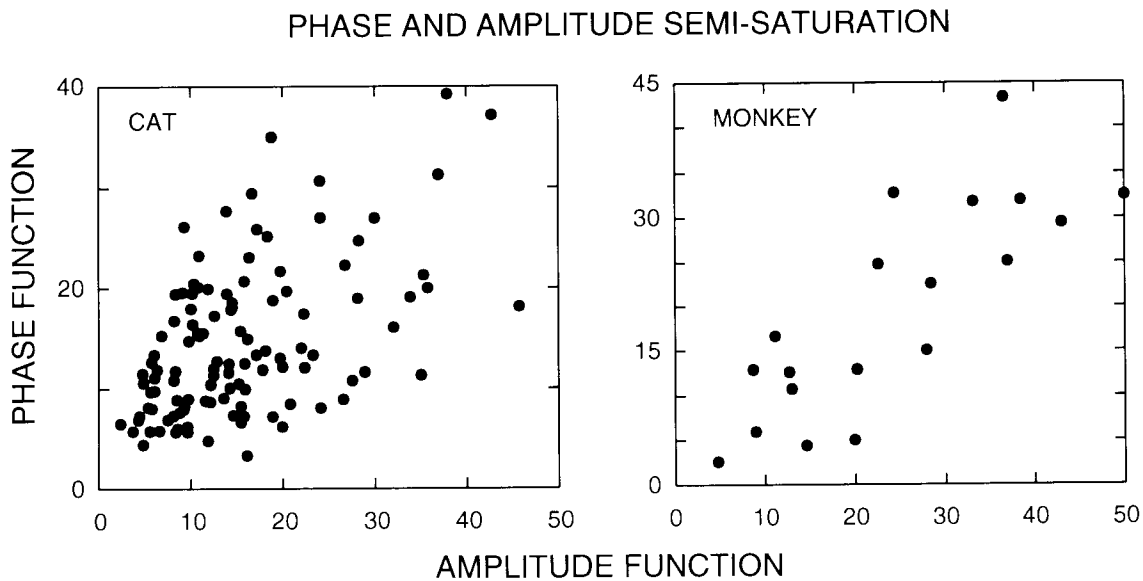


Fig. 7. Scatter plots for the phase and amplitude semi-saturation parameters for the total sample of cells. Each point plots the phase and amplitude semi-saturation for one cell. The values for the amplitude are plotted along the horizontal axis; the values for the phase are plotted along the vertical axis. There was a positive correlation of 0.51 for the cat cells and 0.81 for the monkey cells.



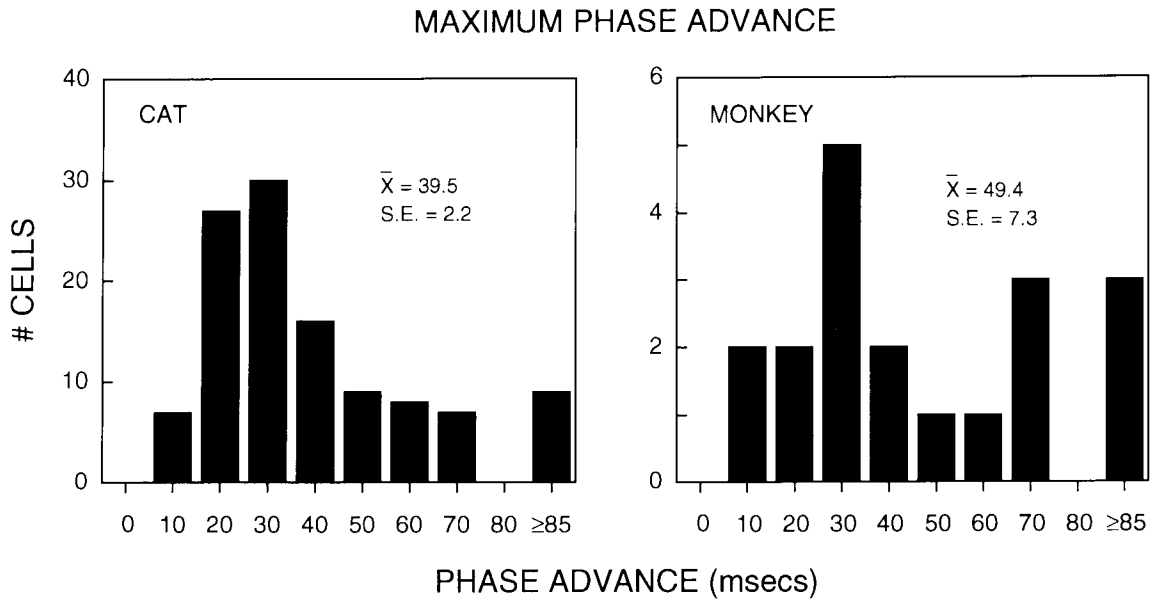


Fig. 8. Distribution of the maximum phase-advance for the entire sample of cells. The  $R_{max}$  parameter indexes the total phase-advance from the lowest contrast measured to the highest contrast measured. The magnitude of the advance varied from cell to cell.

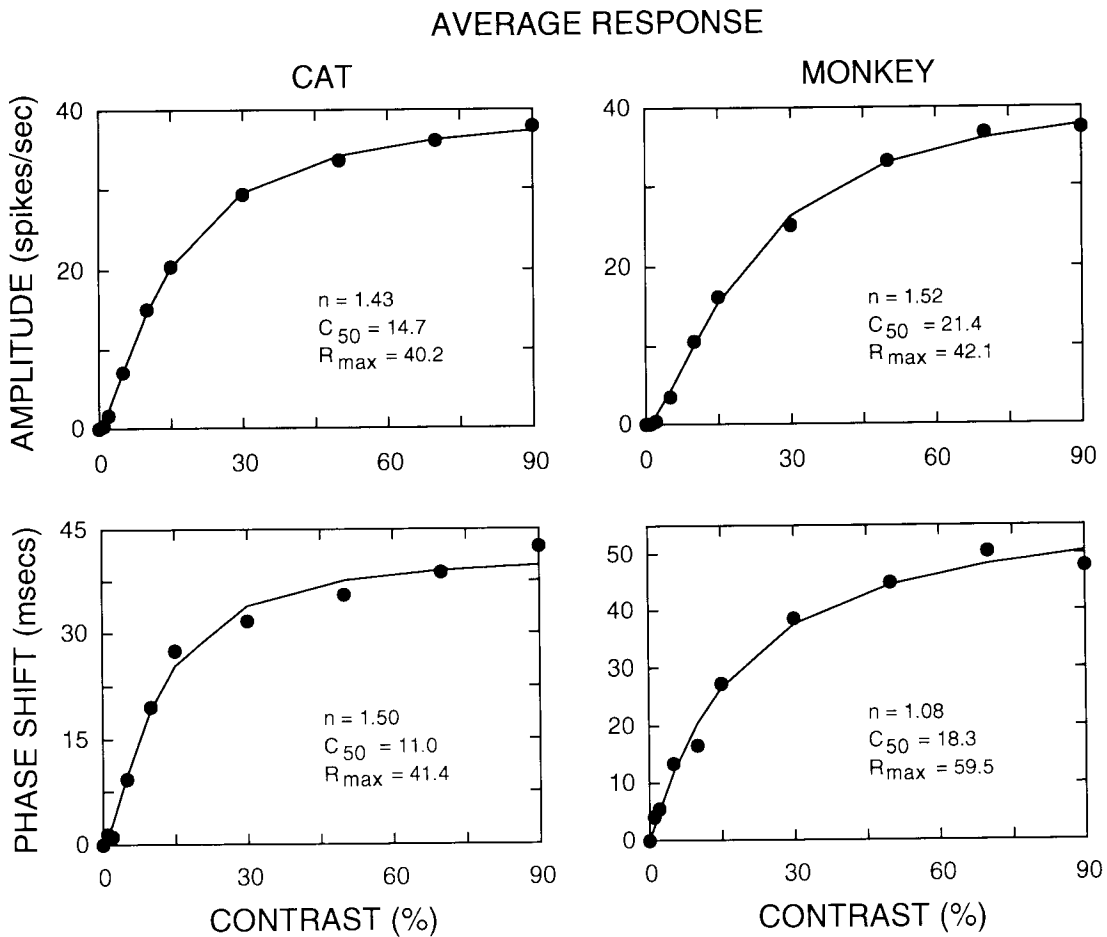
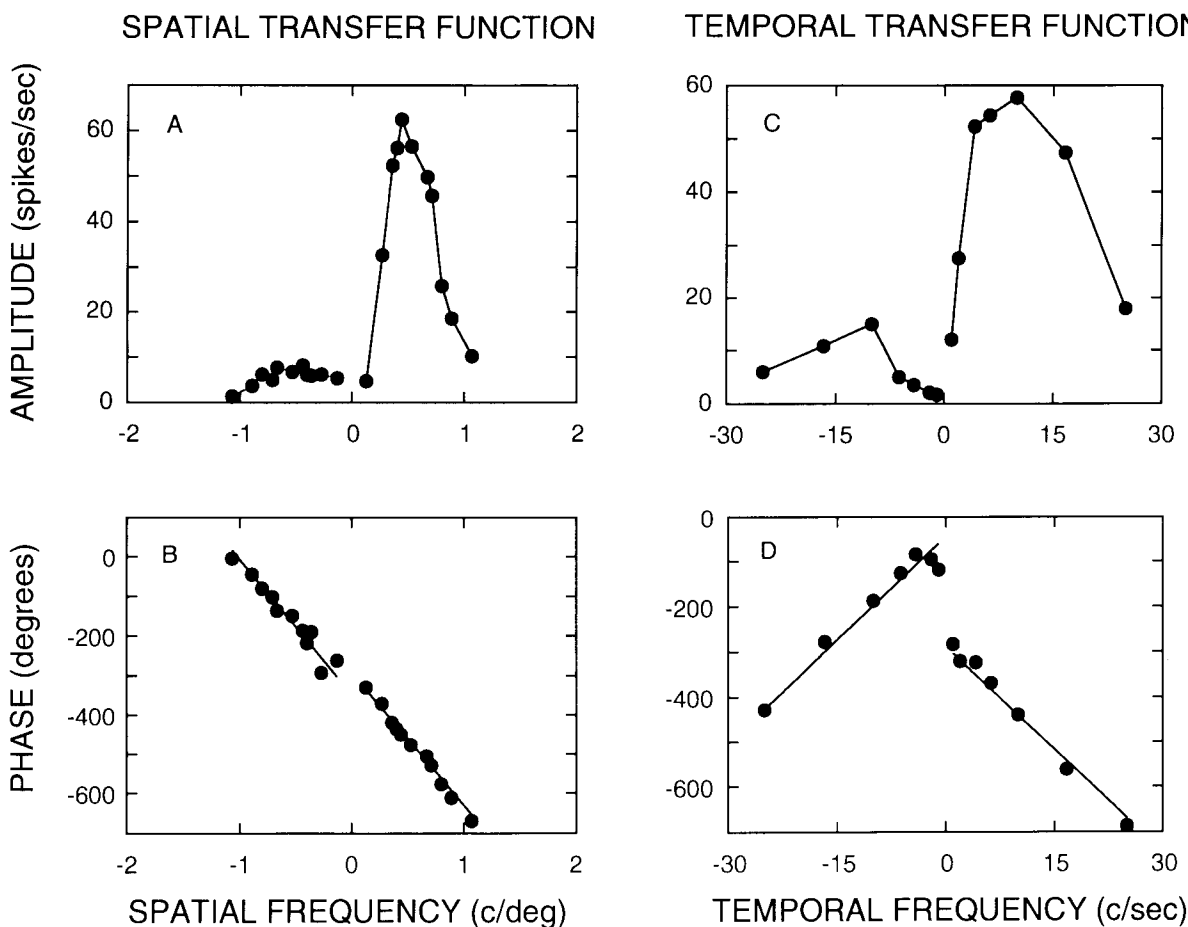


Fig. 9. The average phase and amplitude of the entire sample (measured across a wide range of spatial and temporal frequencies), along with the best fit of eqn. (1).



**Fig. 10.** Spatiotemporal transfer function for a representative neuron (recorded from within the cat visual cortex) measured at a fixed contrast. The amplitude of the response (in spikes/s) and the phase of the response (in deg) are plotted as a function of the spatial frequency and the temporal frequency of a sine-wave grating drifting in the preferred direction of motion (positive frequencies) and in the nonpreferred direction of motion (negative frequencies). The spatial transfer function was measured at 40% contrast and 10.0 cycle/s; the temporal transfer function was measured at 40% contrast and 0.44 cycle/deg. The straight lines through the phase responses show the best fit of a four-parameter linear relationship [see eqn. (2)]. This relationship is composed of a pair of straight lines, one which describes the phase responses as a function of spatial frequency (with odd-symmetry about the origin) and one which describes the phase responses as a function of temporal frequency (with even-symmetry about origin). As can be seen, the phase responses were systematic and they were adequately described by the pair of straight lines. The four parameters of the straight lines index four spatiotemporal properties of the neuron.

spatial frequency and temporal frequency were fitted simultaneously. As can be seen, the phase responses were systematic and they were adequately described by the straight lines of eqn. (2).

Because of the symmetries in the spatiotemporal phase responses, and the fit of eqn. (2), the four parameters of the linear phase relationship can be utilized to describe the observations.

§The phase response measurements were quite reliable. The variance associated with the phase of the response was inversely related to the amplitude of the response and the variance associated with the amplitude. Specifically, as the response amplitude increased, the variance of the amplitude increased (Tolhurst et al., 1983; Geisler & Albrecht, 1995), whereas the variance of the phase decreased. For example, for the cell shown in Fig. 10, the variance of the amplitude was approximately two times larger than the mean. In contrast, the variance of the phase for the largest response was nearly half that of the smallest response: the standard deviation was approximately 20 deg at 60 spikes/s and approximately 40 deg at 6 spikes/s. The standard deviation for all of the phase responses of this cell was approximately 32 deg; this value was typical.

1. There was a fixed time delay of 42.5 ms ( $l = 15.3$ ); this temporal latency introduced a phase-shift which subtracted for motion in the preferred direction, subtracted for motion in the nonpreferred direction, increased as a function of temporal frequency, and was unaffected by spatial frequency.
2. There was a fixed spatial displacement of 0.94 deg of visual angle ( $p = 337.5$ ); this displacement introduced a phase-shift which subtracted for motion in the preferred direction, added for motion in the nonpreferred direction, increased as a function of spatial frequency, and was unaffected by temporal frequency.
3. There was a fixed temporal phase ( $\theta_t = 165.9$  deg); this temporal shape/symmetry introduced a fixed phase-shift which added independent of spatial frequency, temporal frequency, and direction.
4. There was a fixed spatial phase ( $\theta_s = 26.9$  deg); this spatial shape/symmetry introduced a fixed phase-shift which added